

Corrosion tests in water of fuel elements irradiated in the world's first NPP reactor^{*}

Sergey N. Ivanov¹, Sergey I. Porollo¹, Yury D. Baranaev¹, Vladimir F. Timofeev¹, Yury V. Kharizomenov¹

¹ JSC "SSC RF – IPPE" n.a. A.I. Leypunsky, 1, Bondarenko square, Obninsk, Kaluga region, 249033 Russia

Corresponding author: *Sergey I. Porollo* (porollo@ippe.ru)

Academic editor: *Yury Korovin* ♦ **Received** 30 July 2019 ♦ **Accepted** 2 October 2019 ♦ **Published** 10 December 2019

Citation: Ivanov SN, Porollo SI, Baranaev YD, Timofeev VF, Kharizomenov YV (2019) Corrosion tests in water of fuel elements irradiated in the world's first NPP reactor. Nuclear Energy and Technology 5(4): 337–343. <https://doi.org/10.3897/nucet.5.48427>

Abstract

Spent nuclear fuel (SNF) storage in reactor spent fuel pools (SFP) is one of the crucial stages of SNF management technology: it requires special measures to ensure nuclear and radiation safety. During long-term storage in water-filled SFPs, leak-tight canisters in which SFAs are usually placed can become unsealed, which will result in the development of corrosion processes in the fuel element (FE) claddings.

We studied fragments of spent fuel elements of the AM reactor of the World's First NPP during their long exposure in the aqueous medium. The aim of the study was to obtain experimental data on the corrosion changes in the FE claddings and fuel composition during storage as well as on the release of radioactive fission products from them. For the study, a laboratory facility for exposing fuel elements in the water was developed and experimental fragments of fuel elements were made. The study was carried out in the hot chamber of the SSC RF-IPPE. The change in the activity of the water was estimated by the γ -dose rate from the selected water sample. The diameter measurements and metallographic studies were carried out in various sections of FE fragments.

Corrosion tests were carried out on fragments of spent fuel elements of the AM reactor of the World's First NPP that were stored for a long time (more than 50 years – FEs with U-Mo fuel and ~ 20 years – FEs with UO₂ fuel) using standard technology – first in SFP canisters filled with water and then in dry canisters in the air. Placing the fuel elements in the water did not lead to through damage to the FE claddings and a significant change in the size (diameter) of the outer cladding. Metallographic studies of the FE fragments after the corrosion tests showed the presence of intergranular and local frontal corrosion on the surface of the claddings, the depth of which exceeded the depth of the cladding corrosion defects before testing. The rate of radionuclide release from the fuel composition was estimated by the γ -dose rate of water samples taken from the glasses with FE fragments. Throughout the test period, the dose rate of water samples from the glasses with defect-free FEs remained constant. The dose rate from water samples taken from the glasses with the FE fragments with an artificial defect grew during storage.

Keywords

Fuel pin, fuel assembly (FA), spent fuel assembly (SFA), corrosion, defect, aquatic environment, artificial defect, fuel composition, metallographic studies, γ -dose rate, material microstructure, fuel element (FE) claddings, Bilibino NPP

* Russian text published: *Izvestiya vuzov. Yadernaya Energetika* (ISSN 0204-3327), 2019, n. 3, pp. 120–134.

1. Introduction

The fuel assemblies (FA) of the EGP-6 reactor at the Bilibino NPP after irradiation are placed in sealed steel canisters, which are then stored for a long time in the water of the spent fuel pool.

In accordance with current regulatory requirements (NP-016-05 2018, NP-001-15 2018, NP-082-07 2018, NP-091-14 2018, NP-061-05 2018, NP-047-03 2018, NP-004-08 2018, RB-013-2000 2018, NP-002-15 2018, NP-053-04 2018) and safety analysis of handling fuel assemblies, the possibility of failure of a steel canister in the spent fuel pool should be considered.

When water flows from the pool into the unsealed dry canisters, corrosion of the steel claddings of tubular fuel elements begins. This can lead to the appearance of through defects in the claddings, leaching of the fuel composition from the fuel elements and radioactive contamination of the pool water. Quantitative estimates of the rate of this process without the corresponding experimental data are very approximate. Since studies of this kind on the fuel elements of the Bilibino NPP are extremely difficult, analogous fuel elements of the reactor of the World's First NPP reactor were used.

The study was carried out in the hot chamber of the SSC RF-IPPE. The purpose of the study was to obtain data on the behavior of irradiated fuel elements in the water for predictive estimates of the release of radioactive products from fuel elements of the EGP-6 reactor at the Bilibino NPP.

2. Structure and radiation conditions of fuel elements

The fuel elements of the World's First NPP reactor have two coaxially arranged cylindrical claddings made of 1X18H9T stainless steel, between which there is a fuel composition consisting of fuel particles dispersed into a magnesium matrix. The fuel compositions used were U-Mo+Mg or uranium dioxide (UO_2 +Mg). To compensate for axial deformations of the claddings and space the fuel elements in graphite bushings, transverse corrugations 0.3 mm high were applied to the outer claddings of fuel elements containing U-Mo+Mg fuel at a distance of 26 mm. There were no transverse corrugations on the claddings of fuel elements containing uranium dioxide fuel.

The length of the active part of the fuel elements was 1700 mm, the total length was 1885 mm. The outer diameter and thickness of the outer claddings of the fuel elements were 14.0 and 0.2 mm, and of the inner cladding were 9.0 and 0.4 mm, respectively (Ivanov et al. 2011). At the upper and lower ends of the fuel elements there were filling up zones (steel particles in a magnesium matrix) and a plug made of 1X18H9T steel.

The fuel assembly (FA) of the AM reactor consisted of interconnected graphite bushings, in which a central

downtake tube with a diameter of 15 mm and four annular fuel elements were located, in the upper and lower parts connected to peripheral tubes made of 08X18H10T steel. Water flowed through the central tube to the lower distribution chamber, from which it rose upward along the four peripheral tubes of the annular fuel elements, removing heat from the surface of the inner claddings of the fuel elements (Ushakov 1959). During irradiation, the fuel elements were cooled with water at a pressure of 10 MPa, the temperature of the coolant was 150–190 °C at the channel inlet and 210–280 °C at the outlet. The temperature of the outer cladding of the annular fuel element in contact with the graphite channel bushings in the nitrogen medium did not exceed 310 °C (Ivanov et al. 2011).

After irradiation, the fuel assembly was disassembled, the cut fuel elements were placed in steel canisters, which were placed in the spent nuclear fuel (SNF) storage facility.

3. Samples and methods for corrosion tests

For corrosion tests, fuel elements were selected that had been stored in a dry SNF storage facility for a long time. The characteristics of the fuel elements are given in Tab. 1.

Four fragments 395 mm long were cut from the upper and lower parts of the two selected fuel elements. To measure the leaching rate of the fuel composition when in contact with the water, transverse cuts (artificial defects) of $\sim 6.1 \times 3.2$ mm in size and a depth of 0.6 mm were made in the middle part of FE fragments 2 (U-Mo + Mg) and 3 (UO_2 + Mg), while the area of the exposed fuel composition was ~ 8 mm². An artificial defect in Fragment 2 was applied before the start of the corrosion tests, in Fragment 3 after 60 days of testing. Fuel burn-up was determined by the calculation method during operation of FAs in the reactor for the energy production of each FA using standard measurements of the water coolant flow rate and temperature as well as additional measurements by the gamma-spectrometric method from the prepared FE fragments.

To exclude contact of the fuel composition with the air of the hot chamber in the cutting place, the fuel elements were sealed with universal glue and metal plugs. The corrosion tests of the FE fragments were carried out on a specially manufactured facility. During the corrosion tests, the air temperature in the hot chamber was 19– °C, while the underpressure of 20 mm of the water column was maintained in the chamber.

Each of the four fragments of the fuel elements was placed in a separate glass made of steel 20. This material was selected for the glasses because the canisters used to store SFAs in the SNF pool of the Bilibino NPP are made from the same steel. To reduce the evaporation of water during the corrosion tests, lids were put on the glasses.

Table 1. Storage time and burn-up of the studied fuel elements.

Type of fuel composition of FEs	Irradiation period of FEs in the AM reactor	Storage time, years		Fragment No.	Fragment cutting place	Fuel urn-up in a fragment, MW·day/kg
		Total	SNF storage facility			
U-Mo+Mg	1954–1965.	45–55	42	1	0–395 mm from the FE bottom	10.5–13.7
				2	0–395 mm from the FE top	7.7–12.1
UO ₂ +Mg	1988–1992	18–20	16	3	0–395 mm from the FE bottom	9.4–12.3
				4	0–395 mm from the FE top	7.9–12.4

About 300 ml of distilled water was poured into each glass, to which graphite powder weighing ~ 0.5 g was added (to simulate the presence of graphite bushings in the SFAs of the Bilibino NPP).

During the tests, the sealed end of the fragment was always located in the air above the water level in the glass, which eliminated the contamination of the water in the glasses with radioactive fission products through leakages of adhesive sealing. The second end of the FE fragments that was in the water had factory sealing. The water level in the glasses was periodically monitored with a float; the maximum water level was limited by the level of the drain hole in the glass wall. After sampling, water was added to the glasses to the level of the drain hole.

During the corrosion tests, most of the samples, including the factory end parts of the fuel elements, were located in the water, the upper part of the samples in a section 65 mm long was in the air, and a section 15–25 mm long was alternately in the water-air environment (due to the evaporation of water from the glasses).

Periodically (after 30–60 days), the FE fragments were removed from the glasses of the facility for visual inspection and photographing. After that, to determine the activity of water in the glasses, a sample of 10 ml was taken. The corrosion tests of Fragments 2 (U-Mo+Mg) and 3 (UO₂+Mg) with artificial defects were carried out for 430 and 365 days, respectively, after which samples were cut from them for metallographic studies of the condition of the claddings and the fuel composition. The tests of Fragments 1 and 4 lasted for 820 and 760 days, respectively. Before and after the tests, as well as in their course, the diameter of the FE fragments was measured.

4. Water activity measurements

The water activity in each glass was estimated by the γ -dose rate of the selected water sample using an MKS-05 TERRA dosimeter-radiometer. The accuracy of measuring the γ -dose rate of the dosimeter was $\pm 16\%$.

The measurements were carried out in a laboratory room with a background γ -value of 0.15 $\mu\text{Sv/h}$. A measured water sample in a 10 ml test tube was placed close to the dosimeter sensor. For each sample, 20 measurements were performed and the average value of the γ -dose rate was calculated. The measured γ -dose rate of the water from the glasses with FE fragments based on fuel compositions U-Mo+Mg and UO₂+Mg are shown in Figs 1, 2.

The water activity in the samples taken from the glass with sealed FE Fragment 1 with the U-Mo+Mg composi-

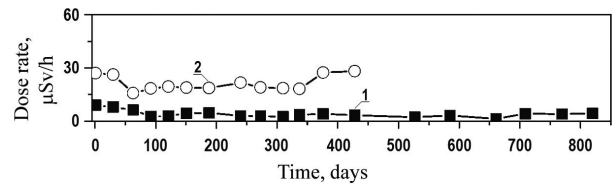


Figure 1. Change in the γ -dose rate of the water in the glasses with the FE fragments based on the U-Mo + Mg composition depending on the test time: 1. Sealed Fragment 1; 2. Fragment 2 with a through defect.

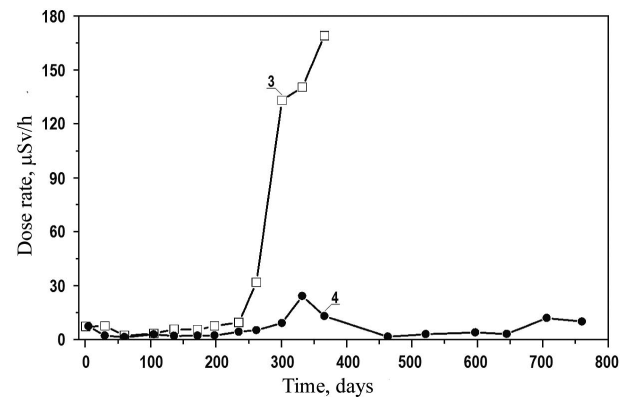


Figure 2. Change in the γ -dose rate of the water in the glasses with the FE fragments based on the UO₂+Mg composition depending on the test time: 3. Fragment 3 with a through defect; 4. Sealed Fragment 4.

tion after 90 days of exposure was established at approximately the same level of $3.3 \pm 1.3 \mu\text{Sv/h}$ (Fig. 1). During periodic inspections of Fragment 1, no damage to its outer cladding was found. The γ -dose rate of the water from the glass with failed FE Fragment 2 with the U-Mo+Mg composition after a small drop at the beginning of the tests gradually increased from 16 to 28 $\mu\text{Sv/h}$ due to the release of radioactive fission products from the fuel via the through defect in the cladding. The water activity level after 430 days of testing in the glass with failed Fragment 2 was approximately nine times higher as compared to the average water activity level in the glass with sealed Fragment 1.

The results of measuring the activity of the water samples from the glass with defect-free FE Fragment 4 with uranium dioxide fuel showed that during most of the tests the γ -dose rate varied from 1.4 to 12 $\mu\text{Sv/h}$ (Fig. 2). A short-term increase in the dose rate to 24 $\mu\text{Sv/h}$ on the 330th day of the test was most likely due to contamination of the selected water samples (due to insufficiently thorough washing of the tube after taking water samples from the glass with failed Fragment 3). The dose rate of

the water samples for the entire time of testing Fragment 4 (with the exception of the short-term rise on the 330th day) averaged $\sim 4.2 \mu\text{Sv/h}$, which is close to the dose rate of the water from the glass with defect-free FE Fragment 1 with U-Mo fuel. This indicates that, for the sealed FE claddings, the water activity was independent of the type of fuel.

After an artificial defect was applied to FE Fragment 3 with UO_2+Mg fuel (60 days after the start of the test), an increase in the water activity was observed: initially it was slow (the gamma dose rate in the first 175 days of defect-water contact increased from 2.2 to $9.6 \mu\text{Sv/h}$), and then it became fast (over the next 130 days of fuel-water contact, the dose rate increased to $171 \mu\text{Sv/h}$). At the end of the tests, the water activity in the glass with the failed FE fragment with UO_2+Mg fuel increased 78 times.

5. Measurements of diameters and examination of FE surfaces

The diameters of the FE fragments were measured with a micrometer in four sections every 100 mm in length with an accuracy of $\pm 0.01 \text{ mm}$. In each section, four measurements were made of the diameter of the fuel element with its rotation relative to the longitudinal axis by 45° .

The measurements showed that the diameters of the outer claddings of Fragments 1 and 4 with the fuel compositions U-Mo+Mg and UO_2+Mg , respectively, did not change during the corrosion tests, the detected diameter changes were within the measurement accuracy. Also, no changes were detected in the diameters of Samples 2 (U-Mo+Mg) and 3 (UO_2+Mg) at the location of the artificial defect.

The surfaces of the FE fragments were examined through binoculars of 10-fold magnification, the characteristic sections of the samples were photographed with a digital camera equipped with a telephoto lens.

Before the corrosion tests, the surface of the claddings of the studied FE fragments was covered with a thin coating of light gray and a small number of tiny spots of dark gray (Fig. 3a, c). During the corrosion tests, various plaques and deposits formed on the surface of the FE fragments (Fig. 3b, d). In the areas of the fragments immersed in the water, tiny dark-gray plaque spots were found, the amount of which increased with the duration of the corrosion tests, as a result of which the surface of the fragments acquired a darker color. After 60 days of the tests, yellow-brown and red-brown (rusty) spots formed on the surface of the FE fragments in contact with water. Deposits of dark gray and black were observed in the areas of the samples located in the lower part of the glass where graphite powder was located. As the test period increased, the number of rust spots and black deposits grew.

In the areas of the FE fragments located near and at the water-air interface in the glasses for corrosion testing (in the zone of the water level change), the largest number of various deposits formed. Deposits of black, white and light gray were observed on the surface of all the FE fragments in these areas, and a yellow or yellow-brown (rus-

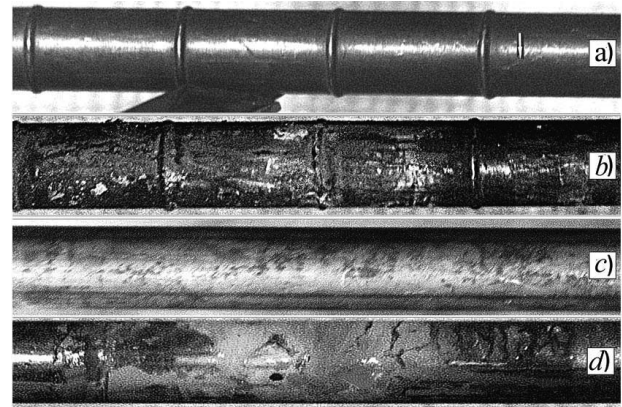


Figure 3. View of the outer surface of the fuel elements: a) Fragment 1 (U-Mo+Mg composition) before the corrosion tests in water; b) Fragment 1 (U-Mo+Mg composition) after the corrosion tests in water for 820 days; c) Fragment 4 (UO_2+Mg composition) before to the corrosion tests; d) Fragment 4 (UO_2+Mg composition) after the corrosion tests in water for 760 days.

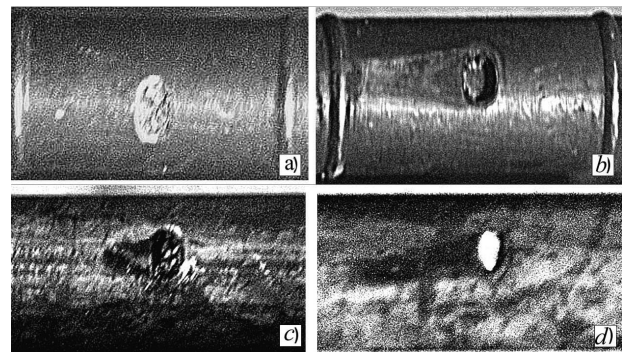


Figure 4. View of the outer surface of the FE fragments with an artificial defect after contact of the fuel composition with water: a) Fragment 2 with the U-Mo+Mg composition after 30 days; b) Fragment 2 with the U-Mo+Mg composition after 165 days; c) Fragment 3 with the UO_2+Mg composition after 75 days; d) Fragment 3 with the UO_2+Mg composition after 170 days.

ty) deposit was also found on the surface of Fragments 1 (U-Mo+Mg) and 4 (UO_2+Mg). The surface appearance of the FE fragments, which was in the air during the corrosion tests, did not change.

The deposits on the FE fragments formed during the corrosion tests were loosely bonded to the surface – when wiped with a cloth swab moistened with an aqueous solution of ethyl alcohol, they were partially or completely removed from the surface of the fragments.

In Sample 2 with U-Mo+Mg fuel, in the artificial defect, only local surface oxidation of the fuel composition was observed (Fig. 4a); after 60 days, leaching of the fuel with the formation of a cavity was detected. After 135 days of testing, a light gray plaque formed on the surface of the cladding around the defect, and after 165 days of testing, the fuel composition of the artificial defect was leached out over the entire thickness of the fuel annulus, while the inner cladding was visible (Fig.4b). In the further tests up to 430 days, the appearance of the artificial defect in Fragment 2 did not change.

In the contact zone of the fuel composition (UO_2+Mg) with the water of FE Fragment 3, the surface of the artificial defect turned dark gray, and a black plaque formed on the surface of the cladding near the defect. After 75 days of contact of the fuel composition with water, a cavity was found at the defect site (Fig. 4c), and after 170 days, the entire surface of the defect turned white (Fig. 4d). In the further tests up to 305 days, the appearance of the defect in Fragment 3 did not change.

6. Metallographic studies

Metallographic studies were carried out in various sections of FE Fragment 2 with U-Mo+Mg fuel and FE Fragment 3 with UO_2+Mg fuel after they were tested in water for 430 and 365 days, respectively. We studied the cross-sections of FE samples located in the water, in the air, in the zone of the water level change in the glass (that is, alternately in the air-water medium) and at the location of the artificial defect.

To determine the initial (before the start of the tests) depth of defects in the claddings, we studied the cross-sections of the fuel elements located near the place where the fragments were cut for the corrosion tests. Microsections were fabricated in a hot chamber according to the standard method, microstructural studies were performed using a MIM-15 remote optical microscope.

During the metallographic studies of the failed FE fragment with the U-Mo+Mg composition after the corrosion tests, we detected pittings, ulcers (10–20 μm deep) (Fig. 5a), intergranular corrosion (up to 15 μm deep) and areas with local frontal corrosion (up to 35 μm deep), while the maximum corrosion depth was observed in the area of the sample located in the water. The depth of corrosion damages on the outer side of the outer cladding before corrosion testing ranged from 5 to 20 μm . Thus, the corrosion tests for 430 days in the water led to the appearance of deeper (by 10–15 μm) corrosion defects, compared with the defects found on the cladding before the corrosion tests. The depth of corrosion ulcers on the inner side of the inner cladding reached 25 μm , which is comparable in magnitude with the corrosion defects on the FE cladding before the corrosion tests. The thicknesses of the outer and inner claddings during the corrosion tests did not change and amounted to 0.20–0.23 and 0.38–0.42 mm, respectively.

When examining the failed FE fragment based on dioxide (UO_2+Mg) fuel after the corrosion tests, we detected ulcers, pittings and areas with local frontal corrosion on the outer side of the FE outer cladding, while the depth of corrosion damages was mainly 2–17 μm (Fig. 5b) and only the depth of individual ulcers was 25–35 μm . The maximum depth of corrosion damages was also observed in the sample area located in the water. The depth of corrosion damages on the outer side of the outer cladding before corrosion testing ranged from 7 to 15 μm . The corrosion tests for 365 days in the water led to the appearance of only a few deeper (by 10–15 μm) corrosion defects, compared

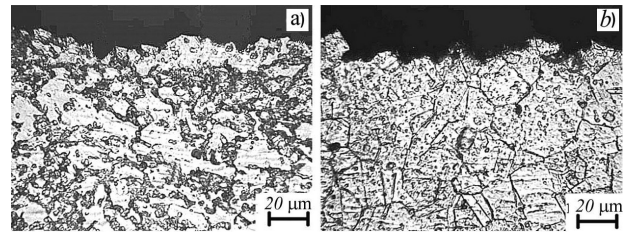


Figure 5. Microstructure of the material on the outer side of the outer cladding of fuel elements with (a) U-Mo + Mg fuel and (b) UO_2+Mg fuel after irradiation, long-term storage, and corrosion tests in an aqueous medium for 430 and 365 days, respectively.

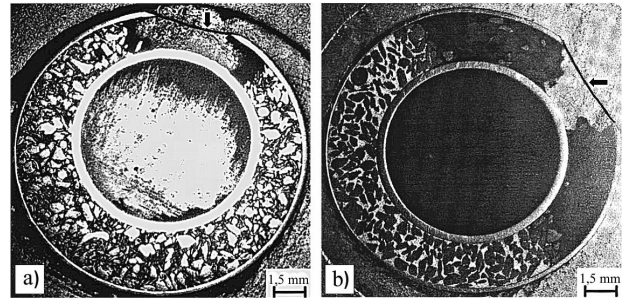


Figure 6. General cross-sectional view of the FE fragments with U-Mo+Mg fuel (a) and UO_2+Mg fuel (b) after testing in water for 430 and 365 days, respectively (arrows indicate the contour of the outer surface of the artificial defect prior to corrosion testing).

with the defects found on the cladding before the corrosion tests. The depth of corrosion damages on the inner side of the inner cladding was 10–15 μm and did not exceed the depth of the corrosion defects observed on the FE cladding before the corrosion tests. The thicknesses of the outer and inner claddings during the corrosion tests did not change and amounted to 0.20–0.21 and 0.38–0.4 mm, respectively.

Figure 6 shows a general cross-sectional view of the FE fragments with fuel compositions based on U-Mo+Mg and UO_2+Mg dioxide at the location of the artificial defect. It can be seen that as a result of exposure to the water in both cases, the fuel composition was leached out via the through defect.

In the UO_2+Mg -based fuel element, sections of the fuel composition adjacent to the edges of the leaching zone were subjected to corrosion, as a result of which the magnesium matrix was oxidized (turned dark gray), and the fuel particles were practically absent as a result of their crumbling during cutting and preparation of the micro-section.

Planimetric measurements showed that in the cross-section of the FE fragment based on a U-Mo+Mg alloy in the defect zone, an area of 9 mm² (or 11% of the total area of the fuel kernel) of the fuel composition was leached out to form a cavity extending in the radial direction throughout the width of the annulus of the fuel element and in the angular direction, in a section with a length of 7.7 mm along its perimeter.

In the cross-section of the FE fragment with the fuel composition based on uranium dioxide (UO_2+Mg), a 5 mm² (or 6.2%) area of the fuel composition was leached

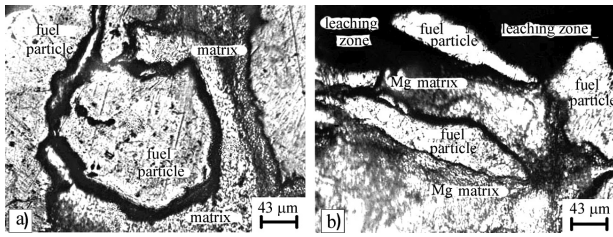


Figure 7. Microstructure of the fuel composition U-Mo+Mg in the cross-section of the artificial defect after testing the FE sample in the water for 430 days: away from the through defect (a) and in the zone of contact with the aqueous medium (b).

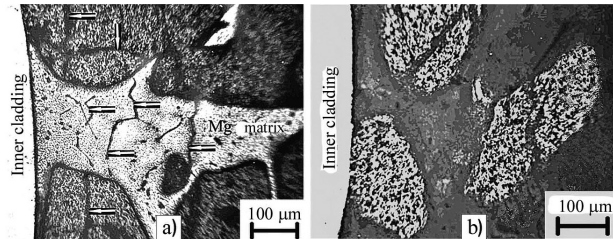


Figure 8. Microstructure of the fuel composition UO_2+Mg in the cross-section of the artificial defect after testing the FE sample in the water for 365 days: away from the through defect (a) and in the zone of corrosion interaction with the aqueous medium (b).

out in the defect zone to form a cavity, the length of which did not exceed the size of the artificial defect. The area of the corrosion zone of the aqueous medium (oxidation) in the FE cross-section was 32 mm^2 (or 39%).

The irradiated fuel composition U-Mo+Mg, after long-term storage and corrosion tests of the FE fragments with the through defect outside the fuel leaching zone, remained intact, and no cracks were found in the fuel grains and magnesium matrix. As a rule, fuel grains are tightly adhered to the matrix, and dark belts with a width of up to $30 \mu\text{m}$ are observed around them (Fig. 7a). In the contact zone of the fuel composition with the water, the magnesium matrix was selectively dissolved, while the fuel grains did not dissolve (Fig. 7b). After the matrix was dissolved around the fuel grains, it was separated from the fuel composition and placed in the cavity, and then, falling into the water, sank to the bottom of the glass, in which the sample with the through defect was located.

The irradiated fuel composition UO_2+Mg after long-term storage and corrosion tests of the FE fragments from the section, where the artificial defect was located, consisted of two parts (Fig. 8).

The first part of the fuel composition, located far from the through defect, was not exposed to the corrosive effects of the water and retained the structure characteristic of irradiated fuel of this type after long-term storage – in the magnesium matrix (light gray, Fig. 8a) and in the fuel particles (dark gray color, Fig. 8a) numerous microcracks were found (shown by arrows), voids were observed around many fuel grains.

The other part of the fuel composition adjacent to the through defect underwent severe corrosion (oxidation) and consisted of a dark gray matrix and a few fuel particles that did not crumble during the manufacture of the microsection (Fig. 8b).

7. Results and discussion

The state of fuel elements after long-term storage is the subject of many studies (Solonin et al. 2000, Volkova et al. 2003, Sidorenko 1993, Ivanov et al. 2000, Golosov et al. 2013, 2013a, INES 2010). In this case, fuel elements with a maximum storage life of 50 years – were subjected to research and testing.

As a result of the corrosion tests of the sealed FE fragments with the compositions U-Mo+Mg and UO_2+Mg in the water for 770–820 days, no damage to the FE claddings was detected. The γ -dose rate of water samples taken from the glasses with the sealed FE fragments remained constant throughout the entire test period. Metallographic studies of the FE fragments after the corrosion tests for 430 days showed the presence of corrosion defects on the cladding surface, the depth of which was $10\text{--}20 \mu\text{m}$ higher than the depth of the cladding corrosion defects before testing. Thus, the accidental ingress of water from the spent fuel pool into dry SFA storage canisters of the EGP-6 reactor at the Bilibino NPP and its contact with sealed fuel elements based on the U-Mo+Mg and UO_2+Mg fuel compositions for 820 and 770 days, respectively, should not lead to their failure and increased water activity in the spent fuel pool.

If in the dry SFA storage canisters there are failed fuel elements with through damage to the cladding, accidental ingress of water from the spent fuel pool into these canisters will increase its activity, while the water activity level in them will depend on both the type of fuel composition and the contact time of water with failed fuel elements.

The water activity in the glass with the failed FE fragment based on uranium dioxide after 305 days of contact with the water was approximately 10 times higher than the water activity in the glass with the failed FE fragment based on U-Mo alloy for the same period. This is due to different mechanisms of the intake of radioactive fission products from these fuel compositions into water. The radioactive fission products only from the volume of the leached fuel composition entered the water in which the FE fragments with the U-Mo+Mg-based fuel composition were tested, while the fission products from the fuel composition based on uranium dioxide also passed from the part of the fuel that had undergone corrosion damage. Due to the presence of microcracks and voids in the fuel composition UO_2+Mg , when the fuel comes into contact with water, it can penetrate through cracks and voids inside the fuel composition, which leads to its oxidation and leaching of fission products from it.

During the interaction between the UO_2+Mg fuel composition and water, radioactive fission products passed from the fuel grains themselves and from the matrix regions around them, where the fission products were concentrated that had escaped or diffused from the fuel particles into the matrix during irradiation and long-term storage. Since the volume of the corroded dioxide fuel composition was significant, this led to a greater intake of fission products from the fuel composition UO_2+Mg and, consequently, to a stronger increase in the water activity than in the case of the fuel composition based on U-Mo+Mg.

The water activity in the glass with the failed FE fragment based on uranium dioxide depends on the duration of water-fuel contact. In the initial period of testing, a slight increase in the activity is observed, but after 175 days of contact with fuel, the activity sharply increases. Therefore, the contact time of irradiated dioxide fuel with water should not exceed 150 days.

8. Conclusion

The claddings of the spent fuel elements with the fuel compositions U-Mo+Mg and UO₂+Mg, after long-term storage and corrosion tests in the aqueous medium for 770–820 days, remained sealed. The depth of corrosion defects on the outer surface of the outer cladding after the corrosion tests for 430 days increased by 10–20 μm,

and no decrease in the thickness of the claddings was detected.

The through defect on the cladding of the FE fragments with the U-Mo+Mg fuel composition and the UO₂+Mg fuel composition caused an increase in the activity of the water by 8.5 and 40 times, respectively, as compared with the activity of the water which was in contact with defect-free fragments.

At the location of the through defect on the fuel elements, leaching of the fuel composition with the formation of a cavity was found. In the fuel element with the fuel composition UO₂+Mg, a zone was observed around the cavity in which corrosion of the magnesium matrix occurred under the influence of water. The formation of this zone led to a greater release of radioactive fission products into the water, the activity of which was 10 times higher as compared to the water activity of the failed FE fragment with the U-Mo + Mg fuel composition.

References

- Golosov OA, Nikolkin VN, Lutikova MS (2013) Fractional Content of Corrosion Products of Spent Nuclear Fuel of AMB Reactors. Proc. of the 10th Russian Conference on Reactor Materials, Dimitrovgrad, 27–31 May. NIIAR Publ., Dimitrovgrad, 288–300. [in Russian]
- Golosov OA, Nikolkin VN, Semerikov VB, Staritsin SV, Bedin VV (2013a) Corrosion of Spent Nuclear Fuel of AMB Reactors. Proc. of the 10th Russian Conference on Reactor Materials, Dimitrovgrad, 27–31 May. NIIAR Publ., Dimitrovgrad, 253–288. [in Russian]
- Ivanov SN, Dvoryshin AM, Popov VV, Shulepin SV (2011) Post-irradiation Tests of Fuel Assembly and Control Rod Channel of the World First NPP. *Atomnaya Energiya* 110(2): 17–70. <https://doi.org/10.1007/s10512-011-9395-3> [in Russian]
- Ivanov SN, Konobeev YuV, Starkov OV, Porollo SI, Dvoriashin AM, Shulepin SV (2000) Material-related Investigation of Fuel Pins Irradiated in the Reactor of Obninsk NPP after 38 Years Storage. *Atomnaya Energiya* 88(3): 183–188. <https://doi.org/10.1007/BF02673157> [in Russian]
- NP-001-15 (2018) General Safety Provisions for Nuclear Power Plants. <https://sudact.ru/law/prikaz-rostekhnadzora-ot-17122015-n-522-ob/np-001-15/> [accessed Oct 10, 2018; in Russian]
- NP-002-15 (2018) Rules for the Safe Management of Radioactive Waste from Nuclear Power Plants. <https://www.seogan.ru/np-002-15-pravila-bezopasnosti-pri-obrashenii-s-radioaktivnimi-otxodami-atomnix-stanciy.html> [accessed Oct 10, 2018; in Russian]
- NP-004-08 (2018) Provisions on the Procedure of Investigation and Accounting of Operational Occurrences at Nuclear Power Plants. <https://gostinform.ru/normativnye-dokumenty-po-atomnomu-nadzoru/np-004-08-obj46450.html> [accessed Oct 10, 2018; in Russian]
- NP-016-05 (2018) General Safety Provisions for Nuclear Fuel Cycle Facilities. <https://normativ.kontur.ru/document?moduleId=1&documentId=89086> [accessed Oct 10, 2018; in Russian]
- NP-047-03 (2018) Nuclear legislation and regulatory documents. Provisions on the Procedure of Investigation and Recording of Events in Operation of Nuclear Fuel Cycle Facilities. <https://sudact.ru/law/prikaz-rostekhnadzora-ot-23122011-n-736-ob/np-047-11/> [accessed Oct 10, 2018; in Russian]
- NP-053-04 (2018) Safety Regulations for Transport of Radioactive Materials. <https://sudact.ru/law/prikaz-rostekhnadzora-ot-15092016-n-388-ob/np-053-16/> [accessed Oct 10, 2018; in Russian]
- NP-061-05 (2018) Safety Rules for Storage and Transportation of Nuclear Fuel at Nuclear Facilities. <https://sudact.ru/law/postanovlenie-rostekhnadzora-ot-30122005-n-23-ob/pravila-bezopasnosti-pri-khranении-i/> [accessed Oct 10, 2018; in Russian]
- NP-082-07 (2018) Nuclear Safety Rules for Reactor Installations of Nuclear Power Plants. http://gostrf.com/norma_data/52/52470/index.htm [accessed Oct 10, 2018] [in Russian]
- NP-091-14 (2018) Safety Ensuring in Decommissioning of Nuclear Facilities. General Provisions. <https://meganorm.ru/Index2/1/4293769/4293769639.htm> [accessed Oct 10, 2018; in Russian]
- RB-013-2000 (2018) RB-013-2000. <https://gostinform.ru/normativnye-dokumenty-po-atomnomu-nadzoru/rb-013-2000-obj52891.html> [accessed Oct 10, 2018; in Russian]
- Sidorenko VA (1993) Conceptual Aspects of Nuclear Power Development to 2010. *Atomnaya Energiya* 76(4): 259–263. <https://doi.org/10.1007/BF02422952> [in Russian]
- Solonin MI, Ioltukhovskiy AG, Velukhanov VP, Kadarmetov IM, Sinelnikov LP, Timokhin AN, Golosov OA, Kuznetsov VR, Tsykanov VA, Pavlov SV, Markov DV, Smirnov VP (2000) Material-related Problems of Long Term Dry and Wet Storage of Spent Nuclear Fuel of RBMK-1000. Proc. of the 6th Russian Conference on Reactor Materials, Dimitrovgrad, 11–15 Sept. NIIAR Publ., Dimitrovgrad 2(2): 3–22. [in Russian]
- INES [The International Nuclear Event Scale] (2010) User's Manual 2010 Edition Jointly Prepared by IAEA and OECD/NEA International Atomic Energy Agency, Vienna. https://howlingpixel.com/i-en/International_Nuclear_Event_Scale [accessed Oct 10, 2018; in Russian]
- Ushakov GN (1959) World's First Nuclear Power Plant (construction and operation experience). Gosenergoizdat Publ., Moscow-Leningrad, 17–19. [in Russian]
- Volkova IN, Grin PI, Kobylansky GP, Lyadov GD, Maershina GI, Novoselov AE, Smirnov VP (2003) State of RBMK-1000 Fuel Pins with E110 Alloy Claddings after Long Wet Storage. Proc. of the 7th Russian Conference on Reactor Materials, Dimitrovgrad, 08–12 Sept. NIIAR Publ., Dimitrovgrad, 2(1): 258–266. [in Russian]